

FROM ANTENNA SPACINGS TO THEORETICAL CAPACITIES - GUIDELINES FOR SIMULATING MIMO SYSTEMS

Laurent Schumacher¹, Klaus I. Pedersen², Preben E. Mogensen²

¹ Center for PersonKommunikation, Niels Jernes vej 12, DK-9220 Aalborg Øst, Denmark, <laurent.schumacher@ieee.org>.

² Nokia Networks, Niels Jernes vej 12, DK-9220 Aalborg Øst, Denmark.

Abstract - Capacity increases promised by Multiple-Input Multiple-Output (MIMO) systems mostly depend on the spatial correlation properties of the radio channel. This paper investigates the connection between these properties and the capacity figures. It first derives the correlation coefficient between two antenna elements as a function of their spacing, the Power Azimuth Spectrum (PAS), the Azimuth Spread (AS) and the mean angle of incidence of the waves, for three different types of PAS, namely uniform, truncated Gaussian and truncated Laplacian. With the help of the established relations, correlated flat-fading MIMO channels are generated, whose capacity performance and Effective Degrees Of Freedom (EDOF) are investigated for two power allocation schemes, water-filling and uniform. The impact of channel estimation errors is also evaluated.

Keywords - MIMO, correlation, capacity, EDOF.

I. INTRODUCTION

For some time now, the concept of Multiple-Input Multiple-Output (MIMO) systems has drawn a lot of attention, up to be listed as a potential improvement of mobile communication systems in standardisation forums [1]. The motivation for this continuously raising interest is the perspective to achieve higher throughputs within a given bandwidth thanks to space diversity schemes [2], [3].

Parallel, orthogonal subchannels are indeed identified in communication systems deploying multiple element antennas at both ends, provided the paths connecting antenna elements of the transmitting end to antenna elements located at the receiving end are uncorrelated [4]. It is well known [5] that an easy way to achieve decorrelation between a pair of antenna elements is to place them away from each other. The exact distance depends on several factors, the level of decorrelation to be achieved, the environment characteristics, etc.

Numerous works published recently have quantified the potential benefits of such MIMO systems, considering various kinds of antenna set-ups placed in a variety of environments, see for instance [6], [7]. How interesting and informative these results might be, they do not enable operators to get a good insight in the factors determining the respective strengths of the parallel subchannels and, consequently, the achievable throughputs. Obviously, one misses guidelines which, starting from the description of the environment and the antenna set-up, would lead to a realistic estimate of the capacity to be achieved.

In fact, many elements requested to establish these guidelines have already been published here and there in the literature. A first purpose of this paper is to combine them in a comprehensive way. This paper also intends to fill in some gaps in these results to address advanced issues, like the spatial clustering of the waves or the impact of channel estimation errors on the evaluation of the capacity.

II. CROSS-CORRELATION FUNCTIONS

The cross-correlation between the waves impinging on two antenna elements has been studied in numerous references. It has been shown that the evolution of the correlation coefficient as a function of the distance between the antenna elements mostly depends on the Power Azimuth Spectrum (PAS) and on the radiation pattern of the antenna elements. Antenna elements will be assumed omnidirectional in the following.

The seminal work of Lee [8] modelled the PAS in outdoor scenarios as the n th power of a cosine function. This model has however been regarded as inconvenient, since it does not enable to derive closed-form expressions [9]. Hence, two other distributions, a truncated Gaussian and a uniform one, have been introduced in [10] and in [11] respectively. More recently, a truncated Laplacian distribution has been proposed in [12] as the best fit to measurement results in urban and rural areas. For these three distributions, namely uniform, truncated Gaussian and truncated Laplacian, the envelope correlation coefficient has been computed as a function of the normalised distance, using the angle of incidence and the Azimuth Spread (AS) as indexing variables.

Unfortunately, these computations do not share a common framework. [9] assumes the Gaussian distribution confined within $[\phi_0 - \frac{\pi}{2}, \phi_0 + \frac{\pi}{2}]$, where ϕ_0 is the mean angle of incidence, while [12] constrains its Laplacian distribution in $[-\pi, \pi]$, assuming the angle of incidence equal to zero thanks to the alignment of the phase origin on the Line-Of-Sight (LOS). The following equations aim at lifting these restrictions by introducing a parameter $\Delta\phi$ such that the PAS is defined over $[\phi_0 - \Delta\phi, \phi_0 + \Delta\phi]$.

Additionally, it has been observed in [13] that the radio waves could gather in several clusters distributed over the space domain. A model of this clustered propagation was introduced in [14]. However, this model misses some freedom, as the spatial clusters are constrained in [14] to have a mean angle of incidence uniformly distributed in $[0, 2\pi]$ and an inner power distributed according to a Laplacian function. This section addresses such multi-cluster situations. The assumption will be that, irrespective of their number, all clusters individually exhibit the same PAS, namely uniform, truncated Gaussian or truncated Laplacian.

A. Uniform PAS

Consider first a multi-cluster uniform PAS modelled as

$$\text{PAS}_U(\phi) = \sum_{k=1}^{N_c} Q_{U,k} \left\{ \begin{array}{l} \varepsilon[\phi - (\phi_{0,k} - \Delta\phi_k)] \\ -\varepsilon[\phi - (\phi_{0,k} + \Delta\phi_k)] \end{array} \right\} \quad (1)$$

where $\varepsilon(\phi)$ is the step function and N_c is the number of clusters. A two-cluster ($N_c = 2$) uniform PAS is shown in Figure 1 ($\phi_0 \in \{-90^\circ, 90^\circ\}$, AS = 30° , $\Delta\phi = 60^\circ$). Its shape is typical of canyon effects [15].

Taking into account potentially power unbalanced clusters, the constants $Q_{U,k}$ are derived such that $\text{PAS}_U(\phi)$ fulfils the requirements of a probability distribution function:

$$\int_{-\pi}^{\pi} \text{PAS}_U(\phi) d\phi = \sum_{k=1}^{N_c} \int_{\phi_{0,k}-\Delta\phi_k}^{\phi_{0,k}+\Delta\phi_k} Q_{U,k} d\phi = 1 \quad (2)$$

which leads to $2 \sum_{k=1}^{N_c} Q_{U,k} \Delta\phi_k = 1$.

Using the notations of [12], with $\frac{d}{\lambda}$ standing for the normalised distance between elements, where d is the element spacing and λ the wavelength, and $D = 2\pi\frac{d}{\lambda}$, one can easily derive the cross-correlation functions between the real and imaginary parts of the complex baseband signals received at two omni-directional antennas separated by a distance d . The cross-correlation function between the real parts, which is the same as the one derived for the imaginary parts, writes

$$R_{XX}(D) \triangleq \int_{-\pi}^{+\pi} \cos(D \sin \phi) \text{PAS}(\phi) d\phi \quad (3)$$

In the case of the uniform PAS (1), the integral leads to

$$\begin{aligned} R_{XX,U}(D) &= J_0(D) \\ &+ 4 \sum_{k=1}^{N_c} Q_{U,k} \sum_{m=1}^{+\infty} \frac{J_{2m}(D)}{2m} \cos(2m\phi_{0,k}) \sin(2m\Delta\phi_k) \end{aligned} \quad (4)$$

where $J_m(\cdot)$ is the Bessel function of the first kind and m^{th} order. On the other hand, the cross-correlation function between a real part and an imaginary one is defined as

$$R_{XY}(D) \triangleq \int_{-\pi}^{+\pi} \sin(D \sin \phi) \text{PAS}(\phi) d\phi \quad (5)$$

which becomes, in the case of the uniform PAS (1)

$$\begin{aligned} R_{XY,U}(D) &= 4 \sum_{k=1}^{N_c} Q_{U,k} \sum_{m=0}^{+\infty} \frac{J_{(2m+1)}(D)}{(2m+1)} \sin[(2m+1)\phi_{0,k}] \\ &\quad \sin[(2m+1)\Delta\phi_k] \end{aligned} \quad (6)$$

From these relations, both field ($\rho_f(D)$) and envelope ($\rho_e(D)$) correlation coefficients are defined as

$$\rho_e(D) \triangleq |\rho_f(D)|^2 \triangleq |R_{XX}(D) + j R_{XY}(D)|^2 \quad (7)$$

The envelope correlation coefficient is shown in Figure 2 as a function of the normalised distance. The coefficient globally decreases with increasing normalised distance. However, oscillations appear during this decrease due to the multi-clustering.

B. Truncated Gaussian PAS

In the case of a multi-cluster Gaussian distribution like in Figure 1, which models as follows:

$$\begin{aligned} \text{PAS}_G(\phi) &= \sum_{k=1}^{N_c} \frac{Q_{G,k}}{\sigma_{G,k}\sqrt{2\pi}} \exp\left[-\frac{(\phi - \phi_0)^2}{2\sigma_{G,k}^2}\right] \\ &\quad \left\{ \begin{array}{l} \varepsilon[\phi - (\phi_{0,k} - \Delta\phi_k)] \\ -\varepsilon[\phi - (\phi_{0,k} + \Delta\phi_k)] \end{array} \right\} \end{aligned} \quad (8)$$

the normalisation constant $Q_{G,k}$ are derived such that

$$\sum_{k=1}^{N_c} Q_{G,k} \text{erf}\left(\frac{\Delta\phi_k}{\sigma_{G,k}\sqrt{2}}\right) = 1 \quad (9)$$

Using definition (8) and normalisation condition (9), the cross-correlation functions are easily derived:

$$\begin{aligned} R_{XX,G}(D) &= J_0(D) \\ &+ \sum_{k=1}^{N_c} Q_{G,k} \sum_{m=1}^{+\infty} \frac{J_{2m}(D) \cos(2m\phi_{0,k})}{\exp(-2\sigma_{G,k}^2 m^2)} \\ &\quad \Re \left[\begin{array}{l} \text{erf}\left(\frac{\Delta\phi_k}{\sigma_{G,k}\sqrt{2}} - jm\sigma_{G,k}\sqrt{2}\right) \\ -\text{erf}\left(\frac{\Delta\phi_k}{\sigma_{G,k}\sqrt{2}} - jm\sigma_{G,k}\sqrt{2}\right) \end{array} \right] \end{aligned} \quad (10)$$

$$\begin{aligned} R_{XY,G}(D) &= \sum_{k=1}^{N_c} Q_{G,k} \sum_{m=1}^{+\infty} \frac{J_{(2m+1)}(D) \sin[(2m+1)\phi_{0,k}]}{\exp[-2\sigma_{G,k}^2 (m + \frac{1}{2})^2]} \\ &\quad \Re \left\{ \begin{array}{l} \text{erf}\left[\frac{\Delta\phi_k}{\sigma_{G,k}\sqrt{2}} - j\sigma_{G,k}\sqrt{2}(m + \frac{1}{2})\right] \\ -\text{erf}\left[\frac{\Delta\phi_k}{\sigma_{G,k}\sqrt{2}} - j\sigma_{G,k}\sqrt{2}(m + \frac{1}{2})\right] \end{array} \right\} \end{aligned} \quad (11)$$

An example of the evolution of the resulting envelope correlation coefficient with respect to the normalised distance is shown in Figure 2 for the multi-cluster truncated Gaussian PAS illustrated in Figure 1. Similar oscillations than the ones observed in the uniform case appear. The decrease of the envelope of these oscillations is however not so quick than in the uniform case. This is a consequence of the more confined profile of the truncated Gaussian PAS compared to the uniform one.

C. Truncated Laplacian PAS

The third type of PAS to be considered is the Laplacian distribution. It has been introduced in [12] as the best fit to measurement results in urban and rural areas. The PAS writes

$$\begin{aligned} \text{PAS}_L(\phi) &= \sum_{k=1}^{N_c} \frac{Q_{L,k}}{\sigma_{L,k}\sqrt{2}} \exp\left[-\frac{\sqrt{2}|\phi - \phi_{0,k}|}{\sigma_{L,k}}\right] \\ &\quad \{\varepsilon[\phi - (\phi_{0,k} - \Delta\phi_k)] - \varepsilon[\phi - (\phi_{0,k} + \Delta\phi_k)]\} \end{aligned} \quad (12)$$

The normalisation condition is given by

$$\sum_{k=1}^{N_c} Q_{L,k} \left[1 - \exp\left(-\frac{\sqrt{2}\Delta\phi_k}{\sigma_{L,k}}\right)\right] = 1 \quad (13)$$

as well as the cross-correlation functions

$$\begin{aligned} R_{XX,L}(D) &= J_0(D) + 4 \sum_{k=1}^{N_c} \frac{Q_{L,k}}{\sigma_{L,k}\sqrt{2}} \sum_{m=1}^{+\infty} \frac{J_{2m}(D)}{\left(\frac{\sqrt{2}}{\sigma_{L,k}}\right)^2 + (2m)^2} \cos(2m\phi_{0,k}) \end{aligned}$$

$$\left\{ \begin{array}{l} \frac{\sqrt{2}}{\sigma_{L,k}} + \exp\left(-\frac{\Delta\phi_k\sqrt{2}}{\sigma_{L,k}}\right) \\ \left[\begin{array}{l} 2m \sin(2m\Delta\phi_k) \\ -\frac{\sqrt{2}}{\sigma_{L,k}} \cos(2m\Delta\phi_k) \end{array} \right] \end{array} \right\} \quad (14)$$

$$R_{XY,L}(D) = 4 \sum_{k=1}^{N_c} \frac{Q_{L,k}}{\sigma_{L,k}\sqrt{2}} \sum_{m=0}^{+\infty} \frac{J_{(2m+1)}(D)}{\left(\frac{\sqrt{2}}{\sigma_{L,k}}\right)^2 + (2m+1)^2} \sin[(2m+1)\phi_{0,k}] \left\{ \begin{array}{l} \frac{\sqrt{2}}{\sigma_{L,k}} - \exp\left(-\frac{\Delta\phi_k\sqrt{2}}{\sigma_{L,k}}\right) \\ \left[\begin{array}{l} (2m+1) \sin[(2m+1)\Delta\phi_k] \\ +\frac{\sqrt{2}}{\sigma_{L,k}} \cos[(2m+1)\Delta\phi_k] \end{array} \right] \end{array} \right\} \quad (15)$$

Using these cross-correlation functions, the envelope correlation coefficient is computed and plot in Figure 2 for the typical multi-cluster case discussed in this section. The oscillations observed in the truncated Laplacian case are wider than the ones observed in either uniform or truncated Gaussian case. This is due to the fact that the truncated Laplacian PAS is the most confined one (see Figure 1), which generates higher correlation values than in the two other cases.

III. SIMULATION OF A MIMO CHANNEL

The MIMO model proposed in [16] can be seen as a straightforward extension of the well-known Single-Input Single-Output (SISO) tapped delay line model commonly used to represent SISO mobile radio channels [17]. When moving from SISO to MIMO models, the main difference is that the tap coefficients of the channel model are no longer scalars but matrices whose size depends on the number of antenna elements exhibited at both ends of the MIMO system.

Consider a system with N_{TX} antenna elements at the transmitter and N_{RX} elements at the receiver. Using notations of [16], the MIMO channel can be modelled as

$$\mathbf{H}(\tau) = \sum_{l=1}^L \mathbf{A}_l \delta(t - \tau) \quad (16)$$

where $\delta(t)$ stands for the Dirac function and L is the number of taps of the channel model. Each matrix $\mathbf{A}_l \in \mathbb{C}^{N_{TX} \times N_{RX}}$. Simulating spatial correlation consists in generating the elements of the L matrices \mathbf{A}_l so as to model the spatial correlation properties of the MIMO channel.

The problem is two-fold:

- 1) How to characterise the spatial correlation properties of a MIMO channel while, so far, it has only been question of correlation properties between elements of a single antenna, thus at one end of the link?
- 2) Knowing the correlation properties, how to generate correlated tap coefficients?

In [16], it has been suggested to model the spatial correlation properties of a MIMO system as the Kronecker product of the spatial correlation matrices defined independently at the transmitter (\mathbf{R}_{TX}) and at the receiver (\mathbf{R}_{RX}):

$$\mathbf{R} \triangleq \text{vec}(\mathbf{H})^H \text{vec}(\mathbf{H}) = \mathbf{R}_{TX} \otimes \mathbf{R}_{RX} \quad (17)$$

whose elements are correlation coefficients, where $(\cdot)^H$ is the conjugate transpose and the $\text{vec}(\cdot)$ operator rearranges the $N_{TX} \times N_{RX}$ matrix \mathbf{H} into a column vector of size $N_{TX}N_{RX} \times 1$. Such a model has been experimentally validated in [18]. On the other hand, a different correlation matrix \mathbf{R}_l could be defined for each tap. However, it is not believed that such a refinement will be required in most cases, so the time index will be dropped on \mathbf{R} in the following. Finally, note that field correlation coefficients are preferred to the envelope correlation coefficients used in [16] because the latter miss the phase information of the former.

Let \mathbf{a}_l be a column vector of $N_{TX}N_{RX}$ zero-mean complex Gaussian random variables with unitary variance. In [19], the column vector $\tilde{\mathbf{A}}_l = \text{vec}(\mathbf{A}_l)$ is generated from \mathbf{a}_l as $\tilde{\mathbf{A}}_l = \mathbf{C}_l \mathbf{a}_l$. \mathbf{C}_l being the square-root decomposition [20, p. 149] of $\mathbf{\Gamma}_l$ whose elements are

$$\Gamma_l(i, j) = \sigma_{h_{m,n}^{(l)}} \sigma_{h_{p,q}^{(l)}} R(i, j) \quad (18)$$

where $\sigma_{h_{m,n}^{(l)}}$ is the standard deviation of the l th tap of the path connecting transmitting antenna element m to receiving element n , with $m, p \in \{1 \dots N_{TX}\}$, $n, q \in \{1 \dots N_{RX}\}$, $i = mN_{RX} + n$ and $j = pN_{RX} + q$.

To illustrate the proposed method, consider a 8×4 MIMO system ($N_{TX} = 8, N_{RX} = 4$) deploying Uniform Linear Arrays (ULA) with .5-wavelength spacing between their elements at both ends. Two cases, the two-cluster case of Figure 1 and a single-cluster case exhibiting a cluster at $\phi_0 = 0^\circ$, will be considered in the following. In both cases, the transmitter experiences truncated Laplacian PAS(s) defined within $[-60^\circ, 60^\circ]$ and whose AS = 30° , while waves impinge uniformly at the receiver within a similar interval ($\Delta\phi = 60^\circ$, AS = $\frac{60^\circ}{\sqrt{3}} = 34.64^\circ$). With the help of relations of Section II, one can derive the elements of the correlation matrices \mathbf{R}_{TX} and \mathbf{R}_{RX} and use them to compute the performance of the system, as described in the following section.

IV. THEORETICAL CAPACITY AND EDOF RESULTS

A. Theoretical capacity

1) *Uniform Power Allocation:* Without any knowledge of the channel characteristics, the only way to distribute the transmit power is to share it equally on all the N_{TX} transmit antenna elements. Assuming independent transmitted signals, their correlation matrix \mathbf{S}_U writes

$$\mathbf{S}_U = \frac{P_{TX}}{N_{TX}} \mathbf{I} \quad (19)$$

where P_{TX} is the total transmitted power and \mathbf{I} is a $N_{TX} \times N_{TX}$ identity matrix. Defining \mathbf{N} as the correlation matrix of the noise samples at the receiver, the theoretical capacity to be achieved on a channel realisation \mathbf{H} is given by

$$C_U = \log_2 \left[\det \left(\mathbf{I} + \mathbf{N}^{-1} \mathbf{H} \mathbf{S}_U \mathbf{H}^H \right) \right] \quad (20)$$

This relation, and the following companion ones, implicitly assumes a frequency-flat MIMO channel. If the channel were frequency-selective, matrices \mathbf{H} and \mathbf{N} would depend on the frequency, such that the argument of the \det operator in (20) should first be integrated over the transmitting bandwidth [7].

2) *Water-filling Power Allocation:* On the other hand, if the transmitter can estimate the channel \mathbf{H} , the water-filling (WF) scheme described in [21] can be applied. According to this scheme, the power allocated to each subchannel P_n is determined to maximise the capacity, given the set of N_λ eigenvalues $\{\lambda_n\}$ of \mathbf{R} . Applying the WF scheme, two expressions of the capacity can be derived. The first one assumes perfect channel estimation whereas the second takes into account channel estimation errors.

With the perfect channel estimate, the correlation matrix of the transmitted signal \mathbf{S}_W , including transmit weights, writes

$$\mathbf{S}_W = \mathbf{V} \mathbf{P}_W \mathbf{V}^H \quad (21)$$

where \mathbf{V} is the matrix of eigenvectors of \mathbf{H} . \mathbf{P}_W is a $N_{TX} \times N_{TX}$ diagonal matrix whose elements are the loading powers of the parallel subchannels derived from the water-filling scheme. The capacity C_W is then obtained as

$$C_W = \log_2 \left[\det \left(\mathbf{I} + \mathbf{N}^{-1} \mathbf{H} \mathbf{S}_W \mathbf{H}^H \right) \right] \quad (22)$$

Taking into account channel estimation errors, the weights to be applied to the transmitting antenna elements are given by \mathbf{V}_ε , the matrix of eigenvectors of $\hat{\mathbf{H}} = \mathbf{H} + \Delta \mathbf{H}$, and the power allocation scheme distributes the power as described by \mathbf{P}_ε , the diagonal matrix of the eigenvalues of $\hat{\mathbf{H}}$, such that the correlation of the transmitted signal writes

$$\mathbf{S}_\varepsilon = \mathbf{V}_\varepsilon \mathbf{P}_\varepsilon \mathbf{V}_\varepsilon^H \quad (23)$$

which leads to the capacity

$$C_\varepsilon = \log_2 \left[\det \left(\mathbf{I} + \mathbf{N}^{-1} \mathbf{H} \mathbf{S}_\varepsilon \mathbf{H}^H \right) \right] \quad (24)$$

The impact of channel estimation errors on the estimation of the capacity has been analytically investigated in [22]. However, the approach in [22] is different from the developments of the present paper, since the transmit power is shared according to the uniform power allocation scheme. The relevancy of this choice for studying the impact of channel estimation errors might be questioned, as this allocation scheme does not rely on any channel estimator. Nevertheless, it has been shown in [22] that the capacity estimation error grows with the Signal-to-Noise Ratio (SNR), the Signal-to-Measurement error Ratio (SMER) and $\min(N_{TX}, N_{RX})$.

3) *Theoretical capacity results:* The cdf of the capacities (20), (22) and (24) are plot in Figure 3 for the 8×4 scenarios. The SNR was chosen equal to 14 dB. The measurement error $\Delta \mathbf{H}$ was modelled as a complex Gaussian white noise, with a SMER $\frac{\sigma_{\Delta \mathbf{H}}^2}{\sigma_{\mathbf{H}}^2}$ set to 3 and 10 dB.

As expected, the capacity delivered by the non-optimal uniform power allocation scheme is smaller than the one achieved with WF. The curves obtained applying WF with mismatched transmit weights seem to lie inbetween. While the WF curve is indeed an upper bound, the uniform should not be regarded as a lower bound of the capacity. Lower SMERs would bring the capacity curves of the mismatched WF below the uniform one, reflecting the fact that allocating all the transmit power to the weakest subchannel is less efficient than sharing it equally between antenna elements. One notices also, as demonstrated in [22], that the estimation error of the capacity increases as the SMER decreases.

Comparing the two scenarios, one can notice that the capacities delivered in the two-cluster case are significantly lower than those

of the single-cluster case. From inspection of the spatial correlation matrices \mathbf{R} , it appears that the MIMO channel is more correlated in the two-cluster case. It makes sense, since the waves impinge from broadside in the single-cluster case ($\phi_0 = 0^\circ$) whereas they arrive from endfire in the two-cluster case ($\phi_0 \in \{-90^\circ, 90^\circ\}$). The parallel subchannels are thus less significant in the latter case, eventually leading to a reduced capacity gain with respect to the more decorrelated single-cluster case. The lower decorrelation of the two-cluster case will be illustrated more clearly in the next subsection.

The outage probability at 10% has been computed as a function of the SNR and is plot on Figure 4. The trends mentioned in the comments of Figure 3 appear here as well. Additionally, the estimation error of the capacity increases with the SNR, as described in [22]. On the other hand, it can also be observed that the slopes of the curves on Figure 4 first increase, then tend to saturate. The following section will focus on this effect.

B. EDOF

To give a better insight in the working of MIMO systems, Effective Degrees Of Freedom (EDOF) have been introduced in [4] as a metric to measure the number of subchannels effectively active. It is given by [7]

$$\text{EDOF}(\text{SNR}) = \left. \frac{dC(x)}{d \log_2(x)} \right|_{x=\text{SNR}} \quad (25)$$

EDOF should converge to $\min(N_{TX}, N_{RX})$ in the case of uncorrelated channels, when the SNR increases. EDOF have been computed for the two scenarios under study, and are plot in Figure 5. The single-cluster case converges indeed to $\min(N_{TX}, N_{RX}) = 4$. However, the two-cluster case saturates at $\text{EDOF} = 3$, which indicates that there are only 3 significant eigenvalues, and thus 3 active subchannels.

V. CONCLUSIONS

This paper has established guidelines to estimate the performance of MIMO systems in terms of theoretical capacity and EDOF from the physical description of the ends of the communication links and the environment. Cross-correlation functions of the received signal at two antenna elements have been derived for three different PASs, namely uniform, truncated Gaussian and truncated Laplacian. Using these relations, a procedure for simulating MIMO radio channels has been described and applied in two case studies. For these two scenarios, theoretical capacity results and EDOF have been computed for two different power allocation schemes, uniform and WF. These results embedded the impact of channel estimation errors. The investigation of the incidence of the mismatch between the transmit weights and the MIMO channel has confirmed that the error of the capacity estimation is getting worse when the SNR increases and when the SMER decreases.

ACKNOWLEDGEMENTS

The authors thank the reviewers for valuable comments. The first author also acknowledges the support of the European Commission under the IST-2000-30148 I-METRA project.

REFERENCES

- [1] 3rd Generation Partnership Project; Technical Specification Group Radio Access Network, "Physical Layer Aspects of UTRA High Speed Downlink Packet Access," Tech. Rep. TR 25.848, 2001.
- [2] G. Raleigh and J. Cioffi, "Spatio-Temporal Coding for Wireless Communications," *IEEE Transactions on Communications*, vol. 46, pp. 357–366, Mar. 1999.
- [3] G. J. Foschini, "Layered Space-Time Architecture for Wireless Communication in a Fading Environment When Using Multi-Element Antennas," *Bell Labs Technical Journal*, vol. 1, no. 2, pp. 41–59, 1996.
- [4] D.-S. Shiu, G. J. Foschini, M. J. Gans, and J. M. Kahn, "Fading Correlation and its Effect on the Capacity of Multielement Antenna Systems," *IEEE Transactions on Communications*, vol. 48, pp. 502–513, Mar. 2000.
- [5] W. Jakes, *Microwave Mobile Communications*. IEEE Press, 1974.
- [6] D. Chizhik, F. Rashid-Farrokhi, J. Ling, and A. Lozano, "Effect of Antenna Separation on the Capacity of BLAST in Correlated Channels," *IEEE Communication Letters*, vol. 4, pp. 337–339, Nov. 2000.
- [7] D. P. Palomar, J. R. Fonollosa, and M. A. Lagunas, "Information-Theoretic Results for Realistic UMTS MIMO Channels," in *Proceedings of IST Mobile Communication Summit 2001*, Sept. 2001.
- [8] W. Lee, "Effects on Correlation Between Two Mobile Radio Base-Station Antennas," *IEEE Transactions on Communications*, vol. 21, pp. 1214–1224, Nov. 1973.
- [9] J. Fuhl, A. F. Molisch, and E. Bonek, "Unified Channel Model for Mobile Radio Systems with Smart Antennas," *IEEE Proceedings - Radar, Sonar Navigation*, vol. 145, pp. 32–41, Feb. 1998.
- [10] F. Adachi, M. Feeny, A. Williamson, and J. Parsons, "Cross-Correlation between the Envelopes of 900 MHz Signals Received at a Mobile Radio Base Station Site," *IEE Proceedings Pt. F*, vol. 133, pp. 506–512, Oct. 1986.
- [11] J. Salz and J. Winters, "Effect of Fading Correlation on Adaptive Arrays in Digital Mobile Radio," *IEEE Transactions on Vehicular Technology*, vol. 43, pp. 1049–1057, Nov. 1994.
- [12] K. I. Pedersen, P. E. Mogensen, and B. H. Fleury, "Spatial Channel Characteristics in Outdoor Environments and their Impact on BS Antenna System Performance," in *Proceedings of IEEE Vehicular Technology Conference VTC 1998, Ottawa, Canada*, vol. 2, pp. 719–723, 1998.
- [13] K. I. Pedersen, P. E. Mogensen, and B. H. Fleury, "A Stochastic Model of the Temporal and Azimuthal Dispersion Seen at the Base Station in Outdoor Propagation Environments," *IEEE Transactions on Vehicular Technology*, vol. 49, pp. 437–447, Mar. 2000.
- [14] Q. H. Spencer, B. D. Jeffs, M. A. Jensen, and A. Lee Swindlehurst, "Modeling the Statistical Time and Angle of Arrival Characteristics of an Indoor Multipath Channel," *IEEE Journal on Selected Areas in Communications*, vol. 18, pp. 347–360, Mar. 2000.
- [15] A. Kuchar, J.-P. Rossi, and E. Bonek, "Directional Macro-Cell Channel Characterization from Urban Measurements," *IEEE Transactions on Antennas and Propagation*, vol. 48, pp. 137–146, Feb. 2000.

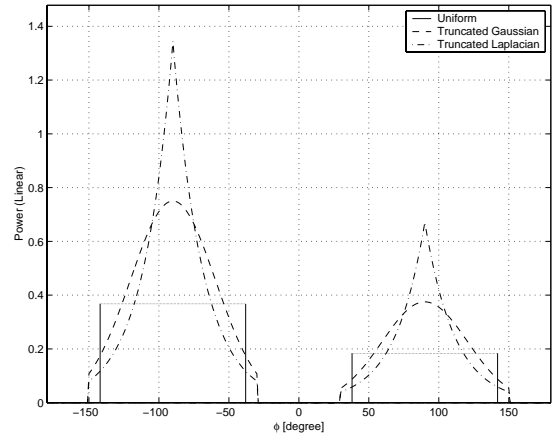


Fig. 1. Normalised PASs for a two-cluster case. For the three PASs, the two clusters have the same AS = 30° but different mean angles of incidence ($\phi_0 \in \{-90^\circ, 90^\circ\}$). Additionally, the 90° cluster has half the power of the -90° one. PASs are confined within $[-60^\circ, 60^\circ]$ intervals.

- [16] K. I. Pedersen, J. B. Andersen, J. P. Kermaol, and P. E. Mogensen, "A Stochastic Multiple-Input-Multiple-Output Radio Channel Model for Evaluation of Space-Time Coding Algorithms," in *Proceedings of IEEE Vehicular Technology Conference VTC'2000 Fall, Boston, MA, USA*, pp. 893–897, Sept. 2000.
- [17] "COST 207 Digital Land Mobile Radio Communications - Final Report," tech. rep., COST 207 Management Committee, 1989.
- [18] L. Schumacher, J. P. Kermaol, F. Frederiksen, K. I. Pedersen, and P. E. Mogensen, "MIMO Channel Characterisation," tech. rep., European IST-1999-11729 Project METRA, Feb. 2001.
- [19] T. Klingenbrunn and P. E. Mogensen, "Modelling Frequency Correlation of Fast Fading in GSM System and Link Level Simulations," in *Proceedings of IEEE 50th Vehicular Technology Conference VTC 1999 Fall, Amsterdam, The Netherlands*, vol. 4, pp. 2398–2402, Sept. 1999.
- [20] G. H. Golub and C. F. Van Loan, *Matrix Computations*. North Oxford Academic, 1983.
- [21] R. Gallager, *Information Theory and Reliable Communications*. Wiley, 1968.
- [22] P. Kyritsi, R. A. Valenzuela, and D. C. Cox, "Effect of the Channel Estimation on the Accuracy of the Capacity Estimation," in *Proceedings of IEEE Vehicular Technology Conference VTC 2001 Spring, Rhodes, Greece*, May 2001.

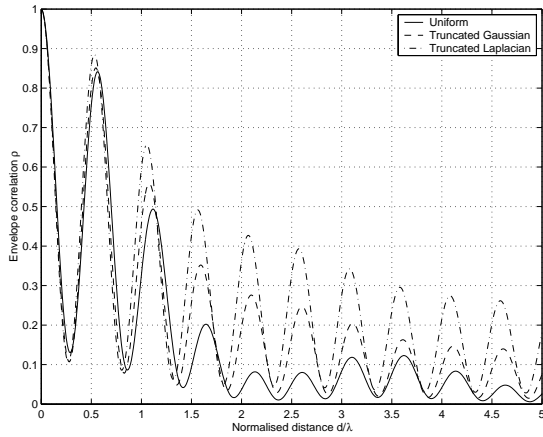


Fig. 2. Envelope correlation coefficient versus the normalised distance for the two-cluster case shown in Figure 1.

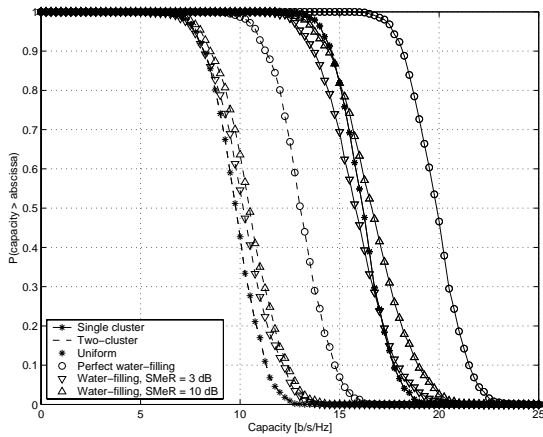


Fig. 3. Complementary cumulative distribution functions of the capacities of the single and two-cluster 8×4 MIMO cases, derived with uniform and water-filling power allocation schemes, assuming either perfect or erroneous channel estimation in the second case.

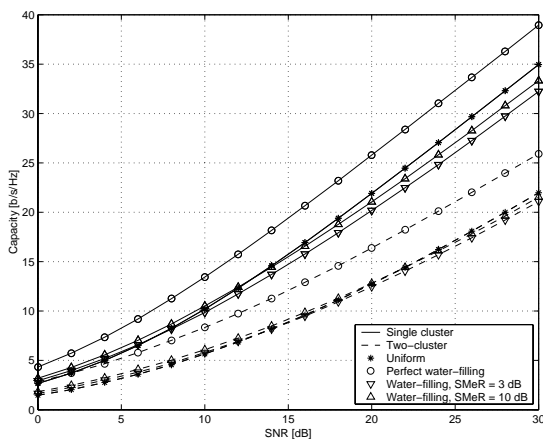


Fig. 4. Outage capacity at 10% of the single- and two-cluster cases as a function of the SNR, for uniform and water-filling power allocation schemes, assuming either perfect or erroneous channel estimation in the second case.

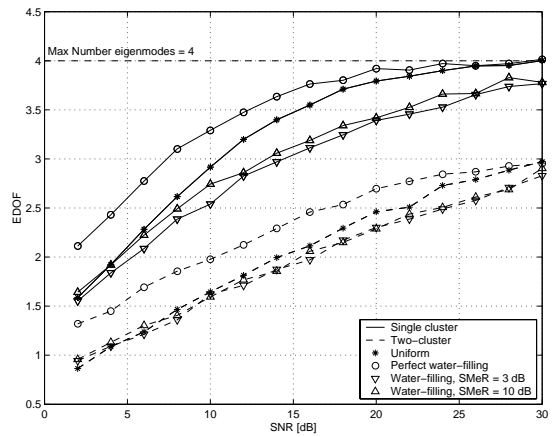


Fig. 5. EDOF of the single- and two-cluster 8×4 MIMO cases as a function of the SNR, for uniform and water-filling power allocation schemes, assuming either perfect or erroneous channel estimation in the second case.